# RECENT ADVANCES IN LOCALIZED COLLOCATION SOLVERS BASED ON SEMI-ANALYTICAL BASIS FUNCTIONS

WENZHI XU & ZHUOJIA FU
Center for Numerical Simulation Software in Engineering and Sciences,
College of Mechanics and Materials, Hohai University, China

ABSTRACT
This paper presents a brief overview of recently developed localized collocation solvers and their various engineering applications. The research progress of localized collocation solvers is discussed, and their basic mathematical formulations are summarized. Finally, applications for thermal analysis in functionally graded materials and steady-state convection-diffusion equation with nonhomogeneous term are given.
*Keywords: localized collocation, semi-analytical basis function, meshless.*

## 1 INTRODUCTION

The finite element method (FEM) is the most widely used numerical technique, but when solving high dimensional, infinite field, and complex-shaped problems, mesh generation and calculation amount become very challenging. The boundary element method (BEM) introduces semi-analytical basis functions as weight functions, and just needs surface mesh, so the calculation amount correspondingly decreases a lot. It is suitable for the solution of the inverse problems, infinite field problems, especially wave conduction problems. But in the BEM, one must evaluate the complex singular and nearly singular integrals, and the resulting interpolation matrix is asymmetric and dense.

To solve the above problems, global semi-analytical meshless collocation solvers are successively proposed, such as the method of fundamental solutions (MFS) [1], radial Trefftz collocation method (RTCM) [2], collocation Trefftz method (CTM) [3], singular boundary method (SBM) [4], and so on. In general, the above-mentioned semi-analytical meshless collocation solvers belong to the family of boundary meshless methods, which avoid the mesh generation. Their approximate solutions are based on the discrete boundary nodes and possess higher accuracy due to the use of the semi-analytical basis functions that naturally satisfy the governing equations. Due to these merits, the global semi-analytical meshless collocation solvers have been successfully used to solve various engineering and science problems.

However, with the demands of large engineering problems, the resulting ill-conditioned interpolation matrices restrict their application. To overcome this challenge, localized collocation solvers (LCSs) [5] are proposed, such as the localized method of fundamental solution (LMFS) [5], [6], localized radial Trefftz collocation method (LRTCM) [7], localized collocation Trefftz method (LCTM) [8], localized singular boundary method (LSBM) [9]. The LCSs can be regarded as a combination of localized collocation schemes [10] and global semi-analytical meshless collocation solvers. They inherit the semi-analytical property from global semi-analytical meshless collocation solvers and avoid the ill-conditioned issue by producing sparse resultant matrices. Localized collocation schemes result in sparse linear systems and the semi-analytical basis functions guarantee high accuracy. Prior to this paper, the LCSs have been successfully applied to various engineering and scientific problems, such


WIT Transactions on Engineering Sciences, Vol 134, © 2022 WIT Press
www.witpress.com, ISSN 1743-3533 (on-line)
doi:10.2495/BE450121

as wave problems [7], heat conduction problems [11], potential-based inverse electromyography [8], in-plane crack problems [12], elasticity problems [5].

The biggest challenge of global semi-analytical meshless collocation solvers is that it is impossible to derive the semi-analytical basis functions of heterogeneous materials. But fortunately, due to the character of localized node collocation, the solution of general heterogeneous problems becomes possible, and also the arbitrary source term can be treated. Based on this, the generalized reciprocity method (GRM) is proposed, which can simultaneously treat heterogeneous materials and arbitrary source terms. The GRM inherits the basic feature of multiple reciprocity method (MRM) [13] which avoids additional internal nodes, and eliminates arbitrary nonhomogeneous terms with only one generalized partial differential operator, which greatly reduces the computational complexity of eliminating complex inhomogeneous terms.

In this paper, the recently developed localized collocation solvers (LCSs), and the correspondingly developed GRM for solving heterogeneous material and heterogeneous source term problems are introduced. The rest of this paper is organized as follows. In Section 2, the basic mathematical formulations of LCSs are presented. Section 3 gives a description of the LCSs in conjunction with the GRM. Section 4 presents two numerical examples and detailed discussion. Finally, some conclusions are summarized in Section 5.

## 2 LOCALIZED COLLOCATION SOLVERS

Consider the following homogeneous boundary value problem

$$\begin{cases} \Re u(\boldsymbol{x}) = 0 \quad \boldsymbol{x} \in \Omega & \text{(1a)} \\ Bu(\boldsymbol{x}) = u_0(\boldsymbol{x}) \; \boldsymbol{x} \in \Gamma & \text{(1b)} \end{cases}$$

where $\Re$ , $B$ are the partial differential operators, $\Omega$ is the computational domain bounded by $\Gamma$ , and $u_0$ is a known function.

In the LCS solution of eqn (1), $N = N_i + N_b$ nodes are distributed inside the computational domain $\Omega$ and along its boundary $\Gamma$ , which is depicted in Fig. 1(a), where $N_i$ is the number of nodes in the computational domain, and $N_b$ is the number of nodes along the boundary. For each selected node $\boldsymbol{x}_1^{(i)} (i = 1, 2, \cdots, N)$ (called central node), the nearest nodes $\left\{ \boldsymbol{x}_j^{(i)} (j = 2, 3, \cdots, m) \right\}$ (called supporting nodes) can be determined easily by Euclidian distance, and the corresponding local subdomain $\Omega_L^{(i)}$ containing *m*-1 supporting nodes is determined (see Fig. 1(b)). To solve eqn (1), in each local subdomain $\Omega_L^{(i)}$, $i$=1,2$\cdots N$ , the following LCSs approximations are considered:

$$u(\boldsymbol{x}_j^{(i)}) = \sum_{s=1}^{m} \alpha_s^{(i)} \mathrm{H}(R_j^{(i)}), \quad \boldsymbol{x}_j^{(i)} \in \Omega_L^{(i)} \quad j = 1, 2, \cdots m, \tag{2}$$

in which, H is the semi-analytical basis function of eqn (1a), $\alpha_s^{(i)}$ are the unknown coefficients, $m$ is the number of source nodes in the local subdomain $\Omega_L^{(i)}$ . $R_j^{(i)}$ is the Euclidian distance corresponding to the collocation node $\boldsymbol{x}_j^{(i)}$ , in the LCTM, it is the distance between the origin and the collocation node $\boldsymbol{x}_j^{(i)}$ . In other LCSs, it is the distance between the source node and collocation node. It should be pointed out that in the LMFS the source

nodes are disturbed outside of the physical boundary and on the physical boundary in other LCSs. In general, the source nodes in the subdomain are the same as the collocation nodes. For the sake of simplicity, eqn (2) is denoted as follows:

$$\boldsymbol{u}^{(i)} = \boldsymbol{D}^{(i)}\boldsymbol{\alpha}^{(i)}, \tag{3}$$

in which, $\boldsymbol{u}^{(i)} = \left[u(\boldsymbol{x}_1^{(i)}), u(\boldsymbol{x}_2^{(i)}), \cdots u(\boldsymbol{x}_m^{(i)})\right]^T$, $\boldsymbol{\alpha}^{(i)} = \left[\alpha_1^{(i)}, \alpha_2^{(i)}, \cdots \alpha_m^{(i)}\right]^T$, $\boldsymbol{D}_{js}^{(i)} = \mathrm{H}(R_j^{(i)})$. By matrix inversion, we have

$$\boldsymbol{\alpha}^i = \left[\boldsymbol{D}^{(i)}\right]^{-1}\boldsymbol{v}^{(i)}, \tag{4}$$

where, $\left[\boldsymbol{D}^{(i)}\right]^{-1}$ is the Moore–Penrose pseudoinverse of matrix $\boldsymbol{D}^{(i)}$.

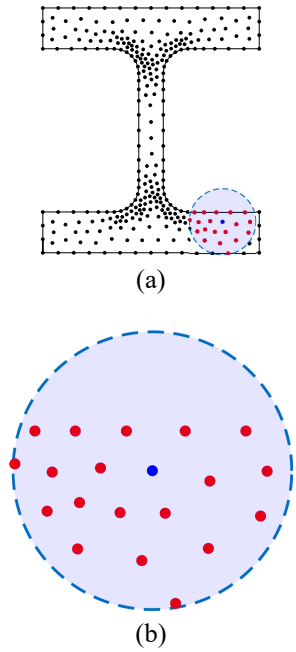

Figure 1: Schematic diagrams of the LRTCM. (a) Node distribution in computational domain; and (b) local subdomain.

Next, for the central node $\boldsymbol{x}_1^i$, we have

$$u(\boldsymbol{x}_1^{(i)}) = \left[\boldsymbol{g}^{(i)}\right]^T\left[\boldsymbol{D}^{(i)}\right]^{-1}\boldsymbol{u}^i = \boldsymbol{K}^{(i)}\boldsymbol{u}^i, \tag{5}$$

where $\boldsymbol{g}^{(i)} = \left[H(R_1^{(1)}), H(R_1^{(2)}), \cdots H(R_1^{(m)})\right]^T$.

For all the interior nodes $(\boldsymbol{x}^{(i)})_{i=1}^{N_i}$ the above eqn (5) is repeated, we have

$$u(\boldsymbol{x}^{(i)}) - \boldsymbol{K}^{(i)}\boldsymbol{u}^{(i)} = 0, \quad i = 1, 2, \cdots N_i. \tag{6}$$

For the $N_b$ boundary nodes $(\boldsymbol{x}^{(i)})_{i=N_i+1}^{N}$ on $\Gamma$, we have

$$B\left(\left[\boldsymbol{g}^{(i)}\right]^T\right)\left[\boldsymbol{D}^{(i)}\right]^{-1} = Bu(\boldsymbol{x}^{(i)}), \quad i = N_i + 1, 2, \cdots N. \tag{7}$$

Finally, combining eqns (6) and (7) and solving the resulting linear system, the approximate solutions of problem (1) at all nodes can obtained. One may find more details about the semi-analytical basis functions in Chen et al. [14].

## 3 GENERALIZED RECIPROCITY METHOD

For the nonhomogeneous boundary value problem

$$\begin{cases} \Re u(\boldsymbol{x}) = f(\boldsymbol{x}) \ \ \boldsymbol{x} \in \Omega \\ Bu(\boldsymbol{x}) = u_0(\boldsymbol{x}) \ \boldsymbol{x} \in \Gamma \end{cases}, \tag{8}$$

the GRM splits the solution of problem (8) into the following two parts

$$u = u_p + u_h, \tag{9}$$

where $u_p$ is the particular solution and $u_h$ is the homogenous solution. The homogenous solution $u_h$ can be easily calculated by the above LCSs. For the particular solution $u_p$, the following equation must be satisfied

$$\Re u_p(\boldsymbol{x}) = f(\boldsymbol{x}) \ \ \boldsymbol{x} \in \Omega.. \tag{10}$$

The nonhomogeneous term $f(\boldsymbol{x})$ can be eliminated by the constructed generalized differential operator $L = \Delta - \dfrac{\Delta f}{f}$, it must be pointed out that the generalized partial differential operator is varied with coordinates. After implementing the generalized differential operator $L$ to eqn (10), the nonhomogeneous term $f(\boldsymbol{x})$ can be eliminated

$$L\Re u_p(\boldsymbol{x}) = Lf(\boldsymbol{x}) = 0 \ \ \boldsymbol{x} \in \Omega.. \tag{11}$$

By solving eqn (11) and obtaining the homogenous solution $u_h$, the solution of nonhomogeneous problem (8) can be found. One can find more technical details for the GRM in Xi et al. [11].

## 4 NUMERICAL RESULTS

In this section, two numerical examples are given to show the effectiveness of LCSs. To assess their performance, the $L_2$ error $Lerr$ and maximum relative error *MRE* are defined:

$$Lerr = \sqrt{\frac{1}{Nt}\sum_{1}^{Nt}\left(\frac{u_{acu}(\boldsymbol{x}_i) - u_{num}(\boldsymbol{x}_i)}{u_{acu}(\boldsymbol{x}_i)}\right)^2}, \tag{12}$$

and

$$MRE = \max_{1 \le i \le Nt}\left|\frac{u_{acu}(\boldsymbol{x}_i) - u_{num}(\boldsymbol{x}_i)}{u_{acu}(\boldsymbol{x}_i)}\right|, \tag{13}$$

where $Nt$ is the number of test nodes, $u_{acu}(\boldsymbol{x}_i)$ and $u_{num}(\boldsymbol{x}_i)$ are the accurate solution and numerical solution, respectively.

### 4.1 LRTCM for the thermal analysis of a 3D functionally circular model

In this Example, the LRTCM is applied to the thermal analysis in a 3D functionally graded peanut model (see Fig. 2). The governing equation is

$$\left((K(\boldsymbol{x})e^{2\boldsymbol{\beta}\bullet\boldsymbol{x}})_{ij}u(\boldsymbol{x})_{,j}\right)_{,i}=0, \qquad \boldsymbol{x}\in\Omega, \tag{14}$$

subject to a Dirichlet boundary condition. The thermal parameters are set as $K=\begin{bmatrix}1 & 0.5 & 0\\ 0.5 & 2 & 0.25\\ 0 & 0.25 & 4\end{bmatrix}$, $\beta_1=0.2$, $\beta_2=0.2$ and $\beta_3=0.3$. The analytical temperature function is

$$u(\boldsymbol{x})=10e^{(-0.2x_1-0.2x_2-0.3x_3)}, \tag{15}$$

from which, the corresponding Dirichlet boundary condition can be derived. In addition, the number of boundary nodes is $N_b=464$ and interior nodes is $N_i=697$.

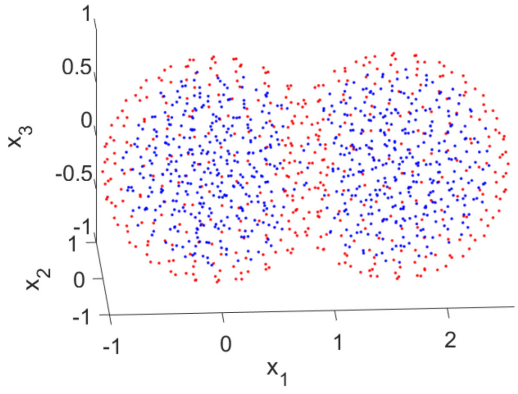


Figure 2: Node distribution of functionally graded peanut model. Red nodes represent boundary nodes and blue nodes represent interior nodes.

Table 1 presents the $L_2$ errors obtained by the LRTCM with different supporting node number S. From Table 1, we can see that the LRTCM with different node number $S\geq 25$ can provide very accurate results, with the increasing supporting nodes the accuracy increases slightly. However, when $S<25$ the LRTCM cannot achieve accurate results. Fig. 3 shows the numerical solution, analytical solution, absolute and relative error distributions by using the LRTCM with S = 30 on the plane $x_3 = 0$. The numerical results given in Fig. 3 show that the LRTCM can obtain very accurate results.

Table 1: Errors with different numbers of supporting nodes with $N = 32627$ total nodes.

| $S$ | 4–24 | 25 | 30 | 40 | 50 | 60 | 70 |
|---|---|---|---|---|---|---|---|
| *Lerr* | / | 5.48E-3 | 2.74E-4 | 2.46E-4 | 2.52E-4 | 3.75E-4 | 2.19E-4 |

Note: "/" means *Lerr* >0.1.

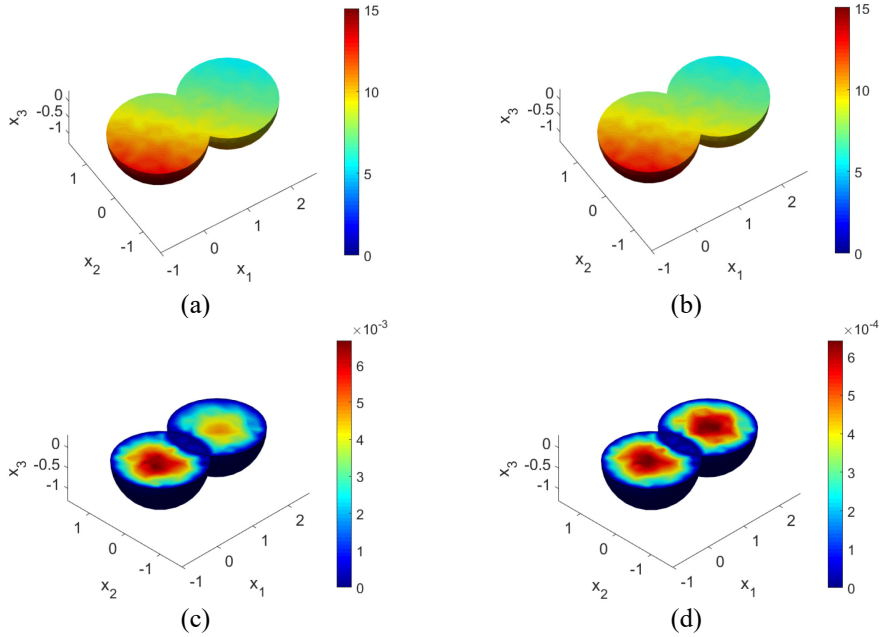


Figure 3: Numerical results of LRTCM for functionally graded peanut model. (a) The numerical solution; (b) The analytical solution; (c) The absolute error; and (d) The relative error.

### 4.2 LMFS and GRM for steady-state convection-diffusion equation with nonhomogeneous term

In this example, the LMFS and GRM are applied to the steady-state convection-diffusion equation with a nonhomogeneous term

$$D\Delta u(\boldsymbol{x}) + \boldsymbol{v}\cdot\nabla u(\boldsymbol{x}) - \lambda^2(\boldsymbol{x}) = f(\boldsymbol{x}), \qquad \boldsymbol{x}\in\Omega, \tag{16}$$

in which $D = x_1 + x_2 + x_3$, $\boldsymbol{v} = [1\ 1\ 1]$, $\lambda(\boldsymbol{x}) = \sqrt{x_1 + x_2 + x_3 + 1}$, and the nonhomogeneous term $f(\boldsymbol{x}) = 2(x_1 + x_2 + x_3 + 1)e^{(x_1+x_2+x_3)}$.

The analytical function is

$$u(\boldsymbol{x}) = e^{(x_1+x_2+x_3)}, \tag{17}$$

from which, the corresponding mixed boundary conditions can be derived. When the coordinate $x_3 > 0.5$, a Neumann boundary condition is imposed, the remain is subjected to a Dirichlet boundary condition. In addition, the number of boundary nodes is $N_b = 1350$ and interior nodes is $N_i = 3375$, while the number of supporting nodes is set to 25. Fig. 4 shows the node distribution of cubic computational domain.

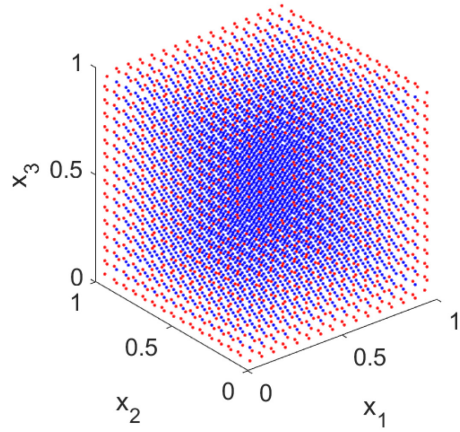


Figure 4: Node distribution of the cubic computational domain.

The generalized partial differential operator $L = \Delta + \dfrac{3(x_1 + x_2 + x_3 + 1)}{(x_1 + x_2 + x_3 + 1)^2}$, the absolute error and relative error on the plane $x_3 = 0.5$ are plotted in Fig. 5, it can be seen that the LMFS performs the very accurate results, the maximum relative error $MRE = 1.95\text{E-}3$. This example shows the feasibility of the LMFS in conjunction with the GRM for solving heterogeneous problems with arbitrary source terms.

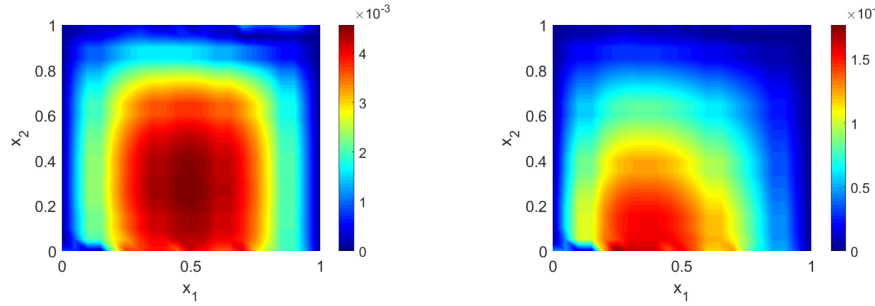


Figure 5: Numerical results of LMFS on the plane $x_3 = 0.5$. (a) The absolute error; and (b) The relative error.

## 5 CONCLUSIONS AND PROSPECTS

In this brief review, recently developed LCSs are introduced. Due to the characteristic of localized node collocation, the ill-conditioned issue is avoided. Heterogeneous problems and heterogeneous source term problems can be also solved by the LCSs with GRM. The two given numerical examples show the ability of the LCSs to analyse heat conduction under functionally graded materials and convection-diffusion equation with nonhomogeneous terms. Overall, it is promised that the proposed LCSs have great potential for engineering applications with heterogeneous materials and arbitrary source terms.

## REFERENCES

[1] Gaspar, C., Some variants of the method of fundamental solutions: Regularization using radial and nearly radial basis functions. *Central European Journal of Mathematics,* **11**, pp. 1429–1440, 2013. DOI: 10.2478/s11533-013-0251-7.

[2] Lin, J., Chen, W., Chen, C.S. & Jiang, X.R., Fast boundary knot method for solving axisymmetric Helmholtz problems with high wave number. *Cmes-Computer Modeling in Engineering and Sciences*, **94**, pp. 485–505, 2013. DOI: 10.1017/S0004972712000810.

[3] Li, Z.C., Lu, T.T. & Hu, H.Y., The collocation Trefftz method for biharmonic equations with crack singularities. *Engineering Analysis with Boundary Elements*, **28**, pp. 79–96, 2004. DOI: 10.1016/s0955-7997(03)00094-8.

[4] Li, W., Chen, W. & Pang, G., Singular boundary method for acoustic eigenanalysis. *Computers and Mathematics with Applications,* **72**, pp. 663–674, 2016. DOI: 10.1016/j.camwa.2016.05.023.

[5] Gu, Y., Fan, C.-M. & Fu, Z., Localized method of fundamental solutions for three-dimensional elasticity problems: Theory. *Advances in Applied Mathematics and Mechanics*, **13**, pp. 1520–1534, 2021. DOI: 10.4208/aamm.OA-2020-0134.

[6] Li, W., Localized method of fundamental solutions for 2D harmonic elastic wave problems. *Applied Mathematics Letters*, **112**, 106759, 2021. DOI: 11210.1016/j.aml.2020.106759.

[7] Wang, F., Gu, Y., Qu, W. & Zhang, C., Localized boundary knot method and its application to large-scale acoustic problems. *Computer Methods in Applied Mechanics and Engineering*, **361**, 112729, 2020. DOI: 36110.1016/j.cma.2019.112729.

[8] Xi, Q., Fu, Z., Wu, W., Wang, H. & Wang, Y., A novel localized collocation solver based on Trefftz basis for potential-based inverse electromyography. *Applied Mathematics and Computation*, **390**, 125604, 2021. DOI: 39010.1016/j.amc.2020.125604.

[9] Wang, F., Chen, Z., Li, P.-W. & Fan, C.-M., Localized singular boundary method for solving Laplace and Helmholtz equations in arbitrary 2D domains. *Engineering Analysis with Boundary Elements,* **129**, pp. 82–92, 2021. DOI: 10.1016/j.enganabound.2021.04.020.

[10] Kamyabi, A., Kermani, V. & Kamyabi, M., Improvements to the meshless generalized finite difference method. *Engineering Analysis with Boundary Elements,* **99**, pp. 233–243, 2019. DOI: 10.1016/j.enganabound.2018.11.002.

[11] Xi, Q., Fu, Z., Rabczuk, T. & Yin, D., A localized collocation scheme with fundamental solutions for long-time anomalous heat conduction analysis in functionally graded materials. *International Journal of Heat and Mass Transfer*, **180**, 121778, 2021. DOI: 18010.1016/j.ijheatmasstransfer.2021.121778.

[12] Gu, Y., Golub, M.V. & Fan, C.-M., Analysis of in-plane crack problems using the localized method of fundamental solutions. *Engineering Fracture Mechanics*, **256**, 107994, 2021. DOI: 25610.1016/j.engfracmech.2021.107994.
[13] Xi, Q., Fu, Z., Alves, C. & Ji, H., A semi-analytical boundary collocation solver for the inverse Cauchy problems in heat conduction under 3D FGMs with heat source. *Numerical Heat Transfer Part B-Fundamentals*, **76**, pp. 311–327, 2019. DOI: 10.1080/10407790.2019.1665386.
[14] Chen, W., Fu, Z.-J. & Chen, C.-S., *Recent Advances in Radial Basis Function Collocation Methods*, Springer, 2014.